Distributions of critical flux: modelling, experimental analysis and consequences for cross-flow membrane filtration

P. Bacchin*, B. Espinasse, P. Aimar

Laboratoire de Génie Chimique, Université Paul Sabatier, 118 Route de Narbonne, 31062 Toulouse Cedex, France

Abstract

This paper discusses the consequences of possible distribution of critical flux (DCF) in cross-flow filtration. These distributions are described here by a normal function with a mean critical flux and its standard deviation. The DCF model allows the description, through an analytical relationship, of the variation in steady state permeate flux with trans-membrane pressure. Both strong and weak forms of critical flux, which can be observed on a membrane operating in cross-flow mode, are depicted. A simple graphical method to determine the mean critical flux and its standard deviation from experimental results is derived from the theoretical model. The theoretical trends are compared to experimental data and show good agreement for cross-flow filtration of latex and BSA suspensions. The distribution function parameters obtained by fitting the DCF model to experiments are compared to critical flux measured via a pressure step method. We thus propose a tool to analyse filtration results and to determine new global parameters for critical conditions (mean value and its standard deviation), which appears to be a good way to account for fouling complexity.
© 2004 Elsevier B.V. All rights reserved.

Keywords: Fouling; Colloid; Ultrafiltration; Microfiltration; Critical flux

1. Introduction

Critical flux is a concept that appeared in the mid 1990s [1–4] to describe the lowest flux for which fouling appears on a membrane. Since then, it has been generally accepted that critical flux represents the permeate flux below which no fouling occurs.

However, such a sharp transition is not often observed in practice and discrepancies between the concept and experiments are observed. Even experimental works carried out with well-characterized suspensions and membranes often exemplify this discrepancy [5,6] and this is further presented in the experimental section of this paper. To take this into account, the concept of critical flux has sometimes evolved by distinguishing a weak form of critical flux from the original strong form of critical flux [7]. The weak form of critical flux

is based on the subtle difference between slow fouling conditions (inducing permeability smaller than that obtained with a clean membrane filtering pure water) and faster fouling (inducing a deviation from the initial linearity of the *J* versus TMP curve). The weak form of critical flux thus shows its ability to describe experiments with numerous fluids from model fluids to complex ones [7]. However, this weak form of critical flux loses the original significance of the previous concept of critical flux and has no direct theoretical grounding.

The main thesis of this paper is to examine if distributions (around a mean value) of critical flux (where critical refers to the strong form of the concept) could be an explanation for behaviour observed during membrane fouling (and the associated weak form of critical flux) and if it could be used as a new tool to interpret filtration data.

In previous studies, the utility of accounting for the distribution of membrane or suspension properties in fouling modelling has already been shown. Yoon et al. [8] reported that when developing a full model accounting for the main

* Corresponding author. Tel.: +33 5 61 55 81 63; fax: +33 5 61 55 61 39.
E-mail address: bacchin@chimie.ups-tlse.fr (P. Bacchin).

transport phenomena, fouling is very sensitive to particle size: the integration of a distribution in particle size can lead to very different fouling simulations. Furthermore, Bowen et al. [9] used the probability distribution function for deposition related to hydrodynamic conditions that they link to randomly distributed protrusion height to describe membrane roughness. This distribution improved the prediction of a Wigner–Seitz cell-based model accounting for multi-body inter-particle interactions. In a recent paper [10], one of us showed that the growth of the boundary layer thickness along a membrane due to hydrodynamic layer development (a form of hydrodynamic conditions distribution) leads to a distribution in local critical flux resulting in a more realistic variation in permeate flux with TMP.

In a first part of the paper, the model for a deposit formation under a distribution of critical flux (DCF) is developed and the effect of a standard deviation around a mean critical flux is investigated. Experimental data of cross-flow ultrafiltration of latex suspensions for different hydrodynamic conditions are interpreted through the DCF model leading to the conclusion that experimental results could be explained by a distribution in critical flux. A comparison of critical flux parameters with experimental determination of critical flux via the pressure step method is further presented. Lastly, the possible origin for critical flux distribution and consequences of the DCF model are discussed. This paper finally gives an explanation for the discrepancy between the "hard theory" of critical flux and "real world" membrane applications.

2. Model for distribution of critical flux (DCF)

The model is based on a normal distribution of critical flux around a mean value (this distribution is justified in Section 4.1). On the other hand, we considered an initial flux (before any fouling), j_0, constant along the membrane. Parameter j_0 is the pure water flux through a clean membrane and is proportional to the applied TMP (trans-membrane pressure); j_0 is used on the *x*-axis of certain figures to describe the effect

of altering the applied TMP. It should be noted at this point that considering a distribution of j_{crit} with a constant j_0 in fact has the same consequence as considering one value of critical flux and a distribution of j_0 (which could be due to local heterogeneity of membrane porosity as discussed in Section 4.1).

2.1. Distribution of critical flux

A normal (or Gaussian) distribution is characterised by the probability density function, pdf(j), or by the cumulative distribution function, cdf(j), as presented in Fig. 1 and defined by the following equations:

$$\text{pdf}(j_{crit}) = \frac{1}{\sigma\sqrt{2\pi}}e^{-((j_{crit}-\bar{j}_{crit})^2/2\sigma^2)} \tag{1}$$

$$\text{cdf}(j) = \int_{-\infty}^{j}\text{pdf}(j_{crit})\,dj_{crit} \tag{2}$$

The probability density function (pdf) is the density of probability such that the probability of the critical flux of being in the interval [*a*; *b*] is given by the integral of this function between *a* and *b*. The pdf function can then give the probability of having a critical flux between two values. The cumulative distribution function (cdf) is then the probability that the critical flux, j_{crit}, is less than or equal to a given flux value j.

2.2. Consequences on fouling conditions

Various fouling regimes can be expected when a run has been started with an initial flux, j_0, if a distribution in critical flux exists. The cdf function calculated for the initial flux j_0 gives the probability of having a critical flux below or above it. Three different situations and their associated probabilities can be determined, as shown in Fig. 2:

- No fouling (nf) if the critical flux is larger than the initial flux ($j_{crit} > j_0$). The probability for such a situation to occur is $p_{nf} = 1 - \text{cdf}(j_0)$.
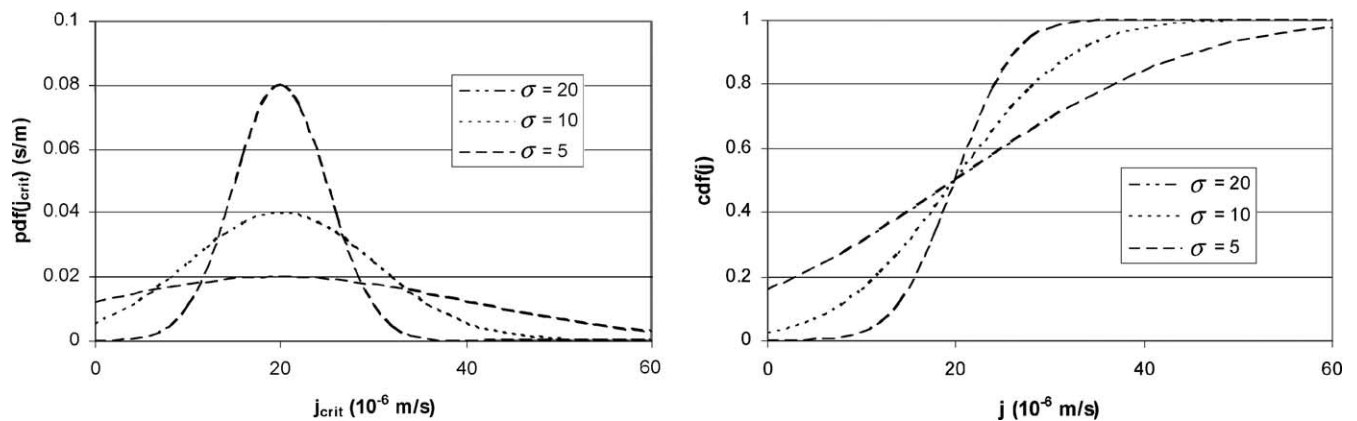

Fig. 1. Normal distribution of critical flux characterised through the probability density function, pdf, and the respective cumulative distribution function, cdf, for the same mean critical flux $\bar{j}_{crit}$ of $20.10^{-6}\,\text{m}\,\text{s}^{-1}$ and three standard deviations σ of 5, 10 and $20.10^{-6}\,\text{m}\,\text{s}^{-1}$.
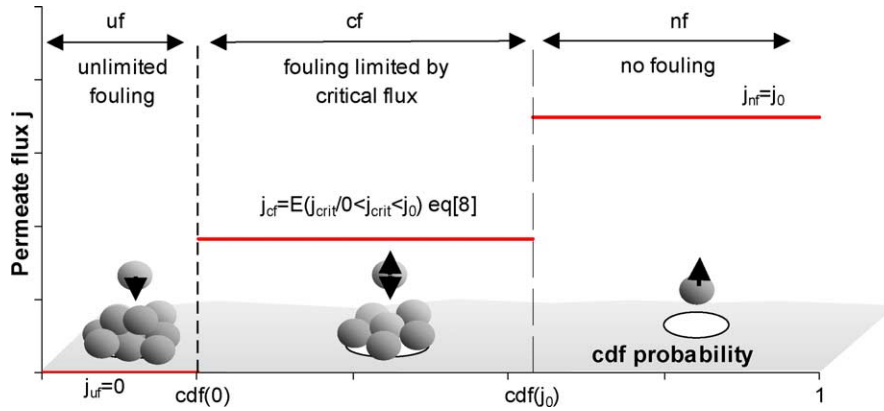
Fig. 2. Probability scale for fouling conditions and associated permeate flux: (1) probability, cdf(0), for unlimited fouling (uf) and permeate flux nil; (2) probability, cdf(j_0) − cdf(0), for fouling limited by critical flux (cf) with a permeate flux given by the expected value of critical flux in Eq. (5); (3) probability, 1 − cdf(j_0), for no fouling (nf) and a permeate flux being the water flux.

- Critical fouling (cf) if the critical flux is smaller than the initial flux but larger than zero ($0 < j_{crit} < j_0$). The probability of this situation is $p_{cf} = \text{cdf}(j_0) - \text{cdf}(0)$.
- Unlimited fouling (uf) if the critical flux is smaller than zero ($j_{crit} < 0$). The probability of this situation is $p_{uf} = \text{cdf}(0)$.

To each of these situations is associated a permeate flux at steady state. In no fouling (nf) conditions, the permeate flux is given by the water flux, $j_{nf} = j_0$. In contrast, for unlimited fouling (uf) conditions, one considers absence of stationary permeate flux and then a permeate flux nil in the steady state, $j_{uf} = 0$, which could correspond to a membrane zone where fouling is continuously increasing (a steady state is not reached) or to complete pore blockage. In the intermediate fouling conditions, where the critical flux is between zero and the pure water flux $0 < j_{crit} < j_0$, fouling is limited by the critical flux (cf) value: it is assumed here that if the water flux overcomes the critical flux then a deposit forms until the flux again reaches the critical value. The resulting permeate flux associated with this event is a "mean" critical flux corresponding to the value of the various possible values of critical flux weighted by their relative probabilities. This "mean" critical flux for these conditions ($0 < j_{crit} < j_0$) is written with the classical function for the expected value $E(j_{crit}/0 < j_{crit} < j_0)$ which is mathematically defined later in Eq. (5). The permeate flux associated with the event (cf) is then equal to the critical flux expected, $j_{cf} = E(j_{crit}/0 < j_{crit} < j_0)$. These three possible fouling conditions control the global permeate flux on the membrane (the sum of their probabilities is equal to one).

2.3. Consequences on the global permeate flux

The resulting global permeate flux, j, through the membrane can be estimated as the sum of the flux of each of the possible situations defined above, weighted by its probability:

$$j = p_{nf} j_{nf} + p_{cf} j_{cf} + p_{uf} j_{uf} \tag{3}$$

Using the probability and the permeate flux as discussed in Section 2.2 leads to:

$$j = (1 - \text{cdf}(j_0)) j_0 + (\text{cdf}(j_0)$$
$$- \text{cdf}(0)) E(j_{crit}/0 < j_{crit} < j_0) \tag{4}$$

The expected value for the critical flux $E(j_{crit}/0 < j_{crit} < j_0)$ which represents the "mean" value of critical flux (in m s^{-1}) when the critical flux is positive and lower that the water flux, is defined as the integral of each possible value of the critical flux, j_{crit}, multiplied by its probability, pdf(j_{crit}), divided by the total probability for this event:

$$E(j_{crit}/0 < j_{crit} < j_0) = \frac{\int_0^{j_0} \text{pdf}(j_{crit}) j_{crit} \, \text{d} j_{crit}}{\int_0^{j_0} \text{pdf}(j_{crit}) \, \text{d} j_{crit}} \tag{5}$$

One can demonstrate (full calculation in Appendix A) using the previous definition of the probability distribution that:

$$E(j_{crit}/0 < j_{crit} < j_0)$$
$$= \frac{\overline{j}_{crit}(\text{cdf}(j_0) - \text{cdf}(0)) - \sigma^2(\text{pdf}(j_0) - \text{pdf}(0))}{\text{cdf}(j_0) - \text{cdf}(0)} \tag{6}$$

The permeate flux is then linked through Eqs. (4) and (6) to the value of the water flux and to the parameters of the critical flux distribution (the mean critical flux, $\overline{j}_{crit}$, and its standard deviation, σ) as follows:

$$j = (1 - \text{cdf}(j_0)) j_0 + \overline{j}_{crit}(\text{cdf}(j_0) - \text{cdf}(0))$$
$$- \sigma^2(\text{pdf}(j_0) - \text{pdf}(0)) \tag{7}$$

This relationship can be used to describe the reduction in flux induced by the fouling under distributed critical conditions. Such a relationship can be easily calculated with a classical spreadsheet program, if the pdf or cdf function is predefined.[1]

Fig. 3 shows the variation in fouling resistance as a function of the water flux (which could also be linked to the TMP)

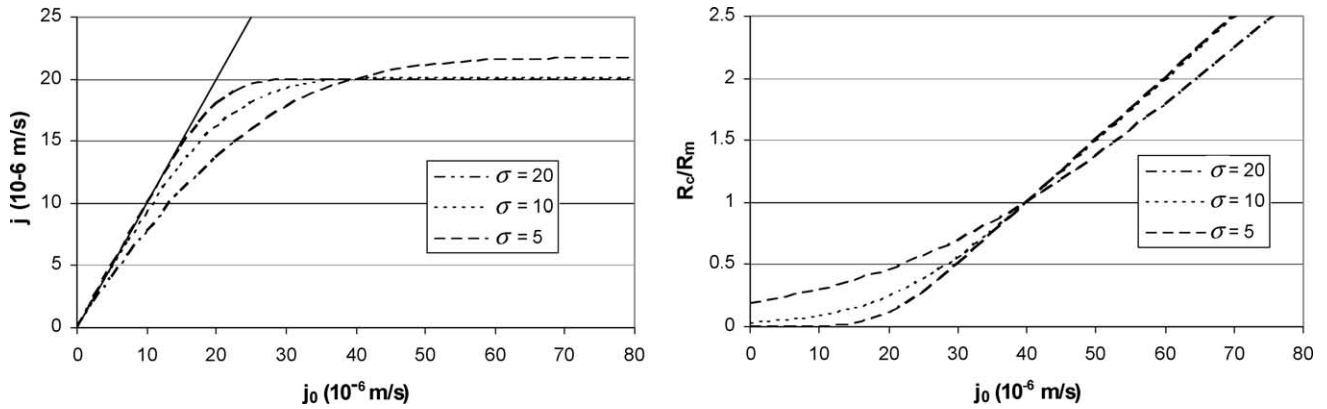---

[1] Spreadsheet program files are available on request.

Fig. 3. Permeate flux (a) and deposit hydraulic resistance (b) vs. water flux. Graphs are plotted for different standard deviations, σ, for a mean critical flux, $\bar{J}_{crit}$, of 20.10^{-6} m s^{-1} corresponding to distributions in Fig. 1.

simulated for the distribution previously presented in Fig. 1. Different fouling behaviours can be described with such a model according the value of the standard deviation. For a low value of standard deviation ($\sigma = 5$), the model depicts a sharp transition between a Darcy behaviour and a pressure-independent regime (strong form of critical flux) with an associated sharp change in cake resistance above the mean value of critical flux. In contrast, for higher values of standard deviation ($\sigma = 10$ and 20), a more gradual transition is observed (weaker form of critical flux).

2.4. Graphic method to determine distribution parameters

Eq. (7), which models the permeate flux, has some particular features shown in Figs. 4 and 5. For small water flux, the limit of Eq. (7) is:

$$\lim_{j_0 \to 0} j = j_0(1 - \text{cdf}(0)) \qquad (8)$$

The slope of the curve "permeate flux versus water flux" tends to $1 - \text{cdf}(0)$ which corresponds to the probability of having a non-nil flux. This can be translated into an initial cake resistance directly linked to the value of cdf(0) as follows:

$$\lim_{j_0 \to 0} \frac{R_c}{R_m} = \frac{1}{(1/(\text{cdf}(0)) - 1} \qquad (9)$$

Such a relationship can be used to determine the initial resistance observable in Fig. 3b from the value of cdf(0) presented in Fig. 1b.

In contrast, for greater water flux, the limit of Eq. (7) is:

$$\lim_{j_0 \to \infty} j = j_{lim} = \bar{j}_{crit}(1 - \text{cdf}(0)) + \text{pdf}(0)\sigma^2 \qquad (10)$$

This relationship shows that when the probability of having reached critical flux tends to one, the flux tends to a limiting value, j_{lim}.

Furthermore, as can be observed in Fig. 3 and derived from Eq. (7), there is a common point for a family of curves with different critical fluxes and standard deviations, which

corresponds to the coordinates $[2\bar{j}_{crit}; \bar{j}_{crit}]$ in Fig. 3a and $[2\bar{j}_{crit}; 1]$ in Fig. 3b.

Also the value of the permeate flux taken for a water flux equals the mean critical flux is:

$$j_0 = \bar{j}_{crit},$$

$$j = \bar{j}_{crit}(1 - \text{cdf}(0)) - \frac{\sigma}{\sqrt{2\pi}} + \sigma^2 \text{pdf}(0)$$

$$= j_{lim} - \frac{\sigma}{\sqrt{2\pi}} \qquad (11)$$

The value of the permeate flux at this point is directly related to the limiting flux and to the value of the standard deviation.

These mathematical properties of Eq. (7) make possible a graphic determination of parameters for critical flux distribution from experimental data of permeate flux versus water flux (or TMP) as shown in Fig. 4. The mean critical flux, $\bar{j}_{crit}$, is given by the y value at the intersection between the "flux versus pressure" curve and the line with a slope which is half that of the initial membrane permeability (point ❶ $[2\bar{j}_{crit}; \bar{j}_{crit}]$ in Fig. 4). Now, the difference between the limiting flux and the flux versus pressure curve at an abscissa $\bar{j}_{crit}$ allows the
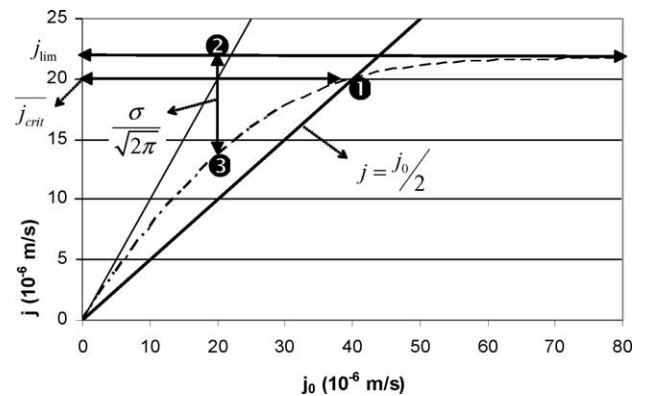

Fig. 4. Graphical method to determine parameters of the distribution in critical flux (mean value, $\bar{J}_{crit}$, and standard deviation, σ) from experimental results (in dashed line) of permeate flux vs. water flux.

value of the standard deviation to be determined according to Eq. (11) (points ❷ and ❸ in Fig. 4).

This method based on the DCF model can be used to determine the mean critical flux and standard deviation from the steady state flux versus pressure plot, if limiting flux is experimentally reachable and if the initial pure water permeability has been measured.

3. Comparison of the DCF model to experimental results

The DCF model is here applied to describe filtration of latex suspensions. Parameters for critical flux distribution are deduced from experiment according to the procedure described in Section 2.4 and are further compared to experimentally obtained critical flux values.

3.1. Material and methods

Filtration experiments were run according to a procedure based on controlled alternating increasing and decreasing pressure steps with the measurements of the steady state flux [5,11]. The steady state flux, automatically detected by the experimental system, has always been measured after filtration periods longer than 30 min. It allows determination of both the classical "steady state" permeate flux versus transmembrane pressure" curve and the fouling reversibility at each step. Such experiments have been performed with latex suspensions (stabilized by charged polyelectrolytes) with a particle size of 106 nm in diameter. Such suspensions have been achieved by dilution in distilled water with a constant latex concentration of 0.7 g/L (which is equivalent to a volume fraction of 5.10^{-4}) both without salt added and with addition of various amounts of KCl. When KCl is added (at 10^{-3} and 10^{-2} M), the total electrolyte concentration is always well below the critical coagulation concentration (c.c.c.) which has been experimentally determined at between 0.1 and 0.3 M in KCl (by observation of settling in a glass cylinder). The addition of salt to some extent controls the repulsive interactions between particles without having inter-particle coagulation in the dilute suspension. The membrane used for these filtrations was M2 Carbosep (Orelis, France) with a molecular weight cutoff of 15 kDa. Different cross-flow velocities have been used between 0.3 and 1.3 m s^{-1} corresponding to Reynolds numbers of 1800 and 7800, respectively. Full results and details on filtration rig and protocols are detailed in [5] and [11].

3.2. Experimental filtration results

In Fig. 5 is plotted the increase in steady state permeate flux versus trans-membrane pressure (with no salt added) for various cross-flow velocities. These experiments show an expected increase in permeate flux when increasing cross-flow velocity. But, no easy and unequivocal observation is possible for the strong critical fluxes in these figures (steady
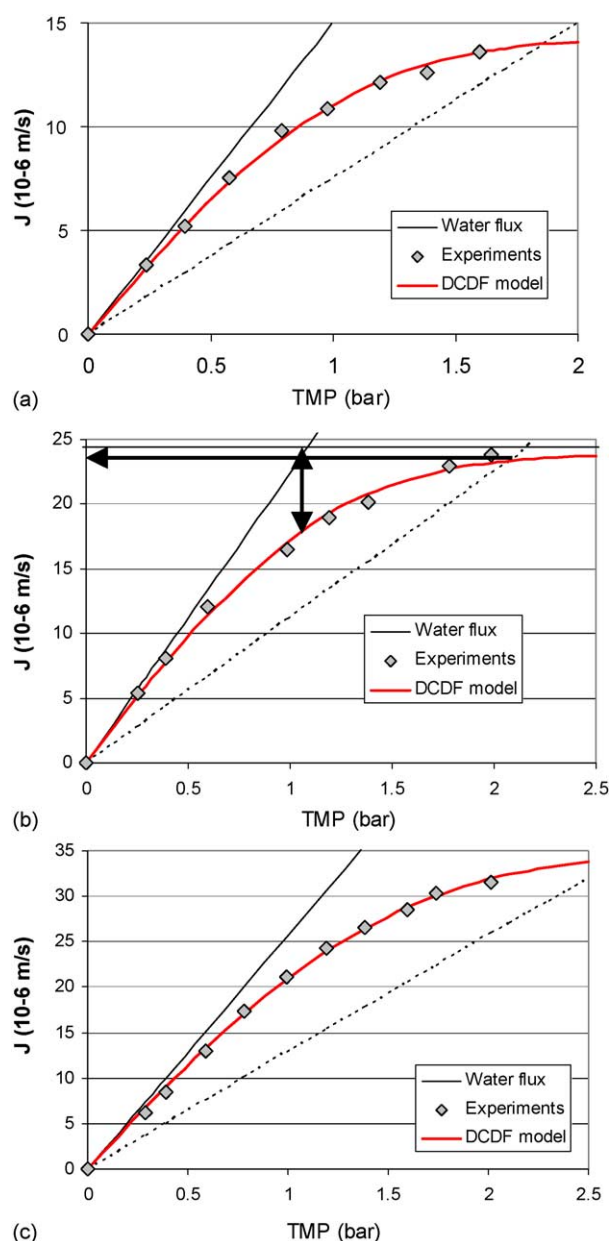

Fig. 5. Permeate flux vs. trans-membrane pressure for three different cross-flow velocities (0.3, 0.6 and 1 m s^{-1} for (a), (b) and (c), respectively). Symbols represent experimental value for latex filtration and bold line DCF model. The dashed line represents the membrane half-permeability.

permeate flux versus TMP) as there is no sharp transition from the Darcy regime to the pressure independent regime. Determining a weak critical flux by determining the point for which there is a deviation from linearity [3] could be very subjective.

In order to have an accurate critical flux measurement, each steady state flux measurement has been followed by a decrease in applied pressure in order to determine the reversibility [5]. This procedure allows a rigorous determination of the critical flux above which irreversible fouling occurs. Table 1 summarizes the results for critical flux obtained with this pressure step method [11]. These results show an

Table 1
Critical flux values ($\times 10^{-6}$ m s^{-1}) experimentally determined with an alternative increasing and decreasing pressure step for different cross-flow velocities, u (m s^{-1}), and ionic strength, I, resulting from KCl addition [16]

	Critical flux ($\times 10^{-6}$ m s^{-1})				
	0.3 m s^{-1}	0.6 m s^{-1}	0.8 m s^{-1}	1.0 m s^{-1}	1.3 m s^{-1}
No salt added	8.9	13	–	19.3	–
$I = 10^{-3}$ M	8.6	10.1	14	–	–
$I = 10^{-2}$ M	–	8.4	–	14.4	18.1

increase in critical flux with the cross-flow velocity and a decrease in critical flux when adding salt. These experiments underline the importance of surface interactions on the critical flux; the critical flux is higher when repulsive surface interactions (stability) are larger as shown in [2]. The critical flux concept which has been theoretically explained by the presence of colloidal surface interactions [2] therefore seems suited to the description of such a system.

3.3. Filtration interpretation through the DCF model

The DCF model has been applied to the experiments shown in Fig. 5. The graphic method detailed in section 2.4 can be used to determine the distribution parameters as plotted in Fig. 5b. The intercept with the membrane half-permeability line (dashed line) gives the value of mean critical flux at around 2.4×10^{-5} m s^{-1}. The value of $\sigma/\sqrt{2\pi}$ can then be determined as 6.5×10^{-6} m s^{-1} which then gives a standard deviation for the distribution, σ, of 1.6×10^{-5} m s^{-1}. With the same model, experimental results have been used to find the mean critical flux and the standard deviation by a classical least square method. Parameters resulting from this numerical optimisation applied to each experiment are presented in Table 2. We can note that graphical and numerical methods give similar results. The agreement between models and experiments is very good when considering both the permeate flux (Fig. 5) and the deposit resistance variations as seen in Fig. 6. The distributions in critical flux involved in the fitting are plotted in Fig. 7 for the three different cross-flow velocities. When increasing the cross-flow veloc-
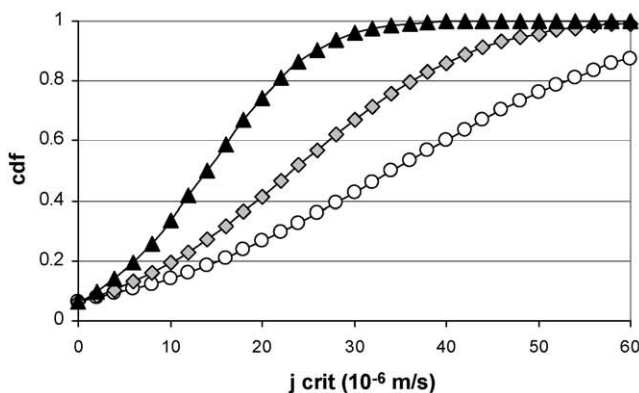
Table 2
Value of mean critical flux, $\overline{J}_{\text{crit}}$, and its standard deviation, σ, ($\times 10^{-6}$ m/s) used to fit latex filtration experiments with DCF model

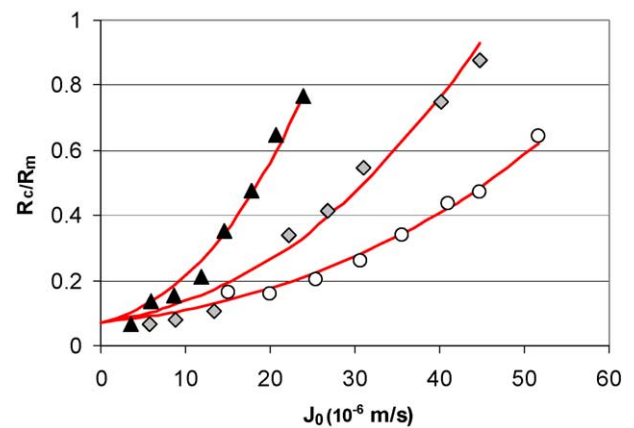|	Critical flux ($\times 10^{-6}$ m s^{-1})				
	0.3 m s^{-1}	0.6 m s^{-1}	0.8 m s^{-1}	1.0 m s^{-1}	1.3 m s^{-1}
No salt added					
$\overline{J}_{\text{crit}}$	13.6	23.3	–	34.1	–
σ	8.21	15.4	–	22.4	–
$I = 10^{-3}$ M					
$\overline{J}_{\text{crit}}$	10	15	19	–	–
σ	5.1	11.6	9.7	–	–
$I = 10^{-2}$ M					
$\overline{J}_{\text{crit}}$	–	12.7	–	18.8	26
σ	–	13.5	–	8.3	13.5

Fig. 6. Deposit hydraulic resistance versus transmembrane pressure. Symbols represent experimental values for latex ultrafiltration and bold lines the DCF model.

ity, one notes an increase in the mean value of critical flux and a distribution which becomes larger. The mean critical flux is multiplied by 2.5 when the cross flow is increased by a factor 3.3 and the standard deviation follows a similar trend.

An explanation for the large distribution in critical flux used for modelling could come, in this paper, from a distribution in the membrane permeability as presented in the
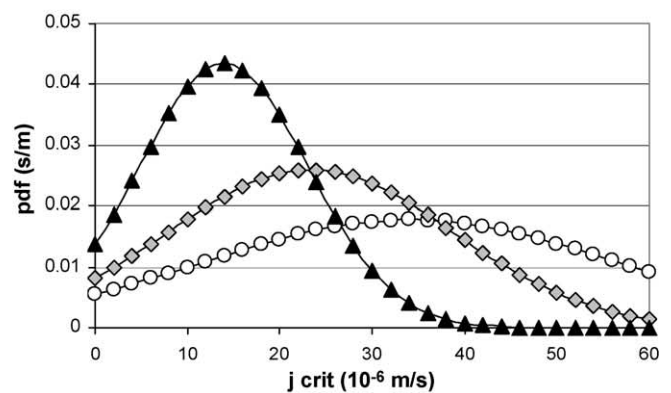

Fig. 7. Normal distribution for critical flux used for the fitting of experimental data presented in Figs. 5 and 6 with the DCF model. Mean critical flux and standard deviations are given in Table 2.
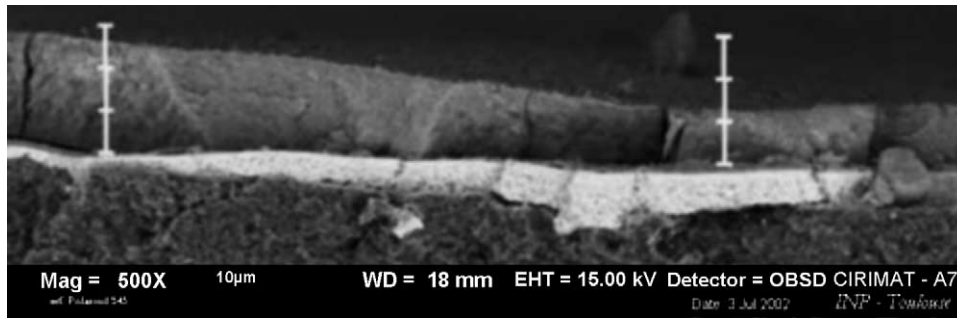
Fig. 8. SEM photograph of a membrane after fouling with a latex suspension. A thin membrane layer (white zone) corresponds to a thick deposit (white vertical bar). The local heterogeneity in porosity can be at the origin of critical flux distributions.

photograph (Fig. 8) showing that the deposit thickness is inversely correlated to membrane skin thickness. Variations in local permeability could then be a possible physical cause for the distribution of critical flux. However, distribution in size or charge of latex particles could also lead to a distribution in stability: the latex suspension exhibited a size distribution centred on 118 nm with a standard deviation of 20 nm when the size analysis (Zetasizer 4, Malvern Inst., UK) was run monomodally (Gaussian distribution). More generally when using the DCF model, numerous sources of distributions can be proposed and some of them are discussed in Section 4.1.

3.4. Comparison of DCF parameters and experimental critical flux

Mean critical flux (Table 2) determined with the DCF model can be compared to results obtained from the experimental determination of critical flux as presented in Section 3.2 (Table 1). A direct comparison (Fig. 9 a)) of experimental critical flux and mean critical flux shows that the experimental critical flux is always lower than the mean critical flux. This gap could be explained by considering that the mean value of critical flux in the distribution corresponds to a probability of 1/2 for reaching critical flux. It could be thought that the experimental detection of critical flux occurs for a probability lower than 1/2 then corresponding to values of permeate flux lower than the mean value of distributed critical flux.

Bearing this in mind, one can seek a link between the experimental critical flux and the mean value, $\bar{j}_{crit}$, and its standard deviation, σ. A rather good agreement is found (Fig. 9b) between the experimental critical flux and the value of the mean critical flux minus half the standard deviation, $\bar{j}_{crit} - (\sigma/2)$. This last value corresponds to a cumulative distribution function, Eq. (2), with a value of 0.3. This could mean that critical flux is experimentally detected when the probability of having a permeate flux larger than the critical flux (i.e. the probability of reaching critical flux) is larger than 0.3. This is illustrated in Fig. 10 where the value of the experimental critical flux (vertical line) is compared to the cumulative distribution function obtained by DCF model (Fig. 7). Again, it can be seen that the pressure stepping method detects a value, which corresponds to the probability of reach-

ing the critical flux of around 0.25 and 0.3. This means that most probably, fouling has already started over some areas of the membrane when we can detect it. This is probably due to the sensitivity of the flux measurements, which measure the average flux over the whole membrane surface, and cannot then detect minute changes in local flux, due to the first irreversible fouling: In line with this remark, the larger the membrane surface, the more difficult the true critical flux will be to determine. On the other hand, the larger the membrane area of the test equipment the more realistic the measured critical flux will be. However, as discussed later on, some of the reasons that the critical conditions are distributed around
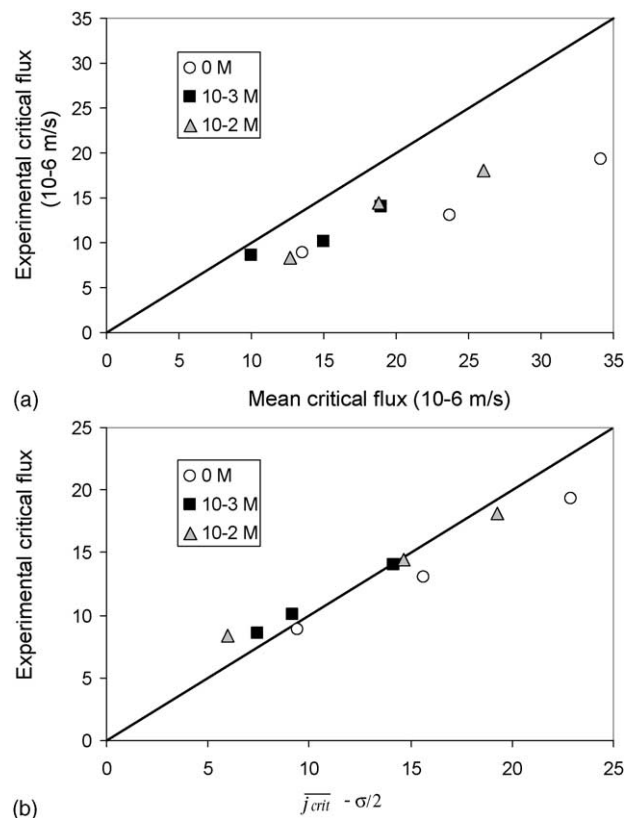

(a)

(b)

Fig. 9. Comparison of the experimental value of critical flux (by a pressure step method [5]) and (a) the mean value of critical flux obtained by the modelling or (b) the mean value minus half of the standard deviation.
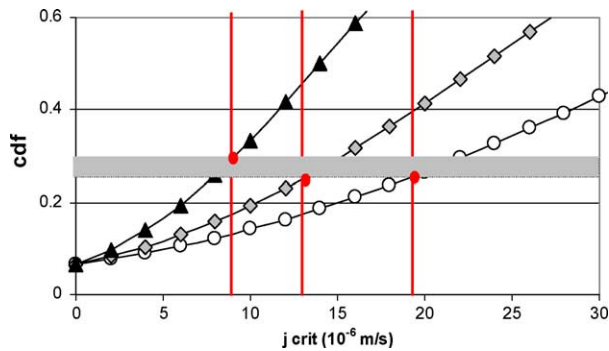
Fig. 10. Position of experimental critical flux (vertical lines) with regard to critical flux distribution deduced from DCF model application (Fig. 7). The experimental detection of the critical flux corresponds for this set of experiments to a probability of having reached the critical value of around 0.25–0.3 (field shading).

a mean value arise from hydrodynamics and from membrane geometries: these parameters, whose exact influence on the distribution is not yet clear, cannot be controlled in such a way that a lab test cell and an industrial plant give the same value for the distribution in critical condition. Hence, there is a risk of significant differences in the extent of fouling between lab tests and real life operation.

If confirmed by further experiments, distribution parameters for fouling conditions could then be linked to the effective critical flux in terms of accumulation reversibility. However, the relationship could be different for other suspensions or membrane properties.

4. Discussions and perspectives

Previous results underline the importance of accounting for the distribution of critical flux (DCF) to interpret filtration results even with a suspension being a priori homogeneous in properties. The ability of a mean critical flux and the relative standard deviation to interpret filtration results and the possibility to link these parameters to the experimental critical flux suggests an interesting use of this model for membrane fouling characterisation and data extrapolation. In this section, we investigate the possible origin of DCF. The link between the DCF model with other existing concepts and theories is briefly discussed.

4.1. Physical basis for distribution of critical flux (DCF)

First, physical causes for the DCF are examined to discuss the theoretical meaning of the model. DCF due to tangential hydrodynamics through the development of the boundary layer has already been investigated [10] and is not included in this section.

The existence of a critical flux (which represents a critical fouling condition in cross-flow filtration) can be shown from modelling based on very different kinds of approaches:

- A mass balance with classical convective and diffusive terms to which is added a term for surface interaction between a colloid and the surface [2].
- A force balance (mechanical) on a particle near the membrane surface [12] which integrates a force induced by multi-body surface interaction.
- A mass balance with a diffusive term based on an osmotic pressure for suspensions with a critical volume fraction (thermodynamic approach) [13] to describe the aggregation phenomena.

From these approaches, the critical flux can then be similarly seen as the consequence of:

- A critical volume fraction of particles (in a thermodynamic approach) resulting from a mass balance between convection and dispersive mass flux and leading to mass "condensation".
- A critical force acting on the particles (in a mechanistic approach) leading to their aggregation (repulsive interaction between particles overcome by permeation) on the membrane.

Generally, the critical condition for fouling can always be reduced to a balance between the convective drag force on the particle (link to the initial flux, j_0), F_{drag} and the dispersive forces F_{disp} as follows:

$$j_0 < j_{crit} \Rightarrow F_{drag} < F_{disp} \Rightarrow \text{no deposit formation} \qquad (12)$$

When dealing with critical flux, one can think that a distribution of both drag force (or relative particle/solvent velocity) and dispersive force (or critical velocity) can occur near the membrane surface. The distribution of drag force can be the result of:

- A distribution in relative particle/solvent velocity near the surface due to multi-body hydrodynamic or colloidal interactions.
- A distribution in solvent velocity (local permeate flux) along the membrane surface because of heterogeneity in pore shape or size or in membrane skin thickness.

The possible causes for distribution in these different parameters (investigated in next section) are sketched in Fig. 11.

4.1.1. Distribution in particle/fluid velocity

Particle velocity distributions caused by multi-body hydrodynamic interactions have been studied by numerical simulation [14–15]. As an example, the fluctuation of velocity around a mean value during settling of a concentrated suspension follows a Gaussian distribution [14]. The fluctuation can then be considered as a "diffusion-like" motion even if the causes for the distribution are purely hydrodynamic in nature. By analogy with settling (particles moving in an immobile fluid), this kind of distribution can also take place in a filtration process under the form of a distribution in relative particle/fluid velocity of (and then drag force on) a particle
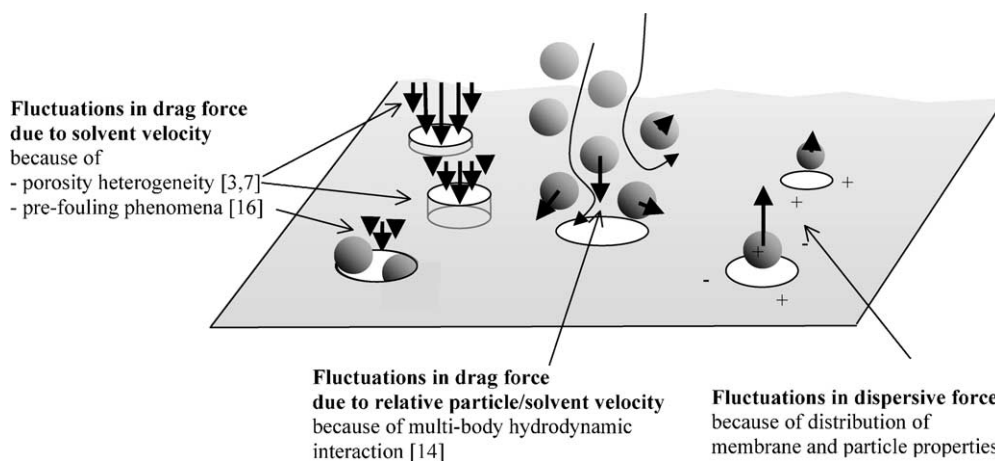
Fig. 11. Various possible origins for fluctuations in the drag force and dispersive force balance on a particle near a membrane surface.

immobilised near a membrane surface and dragged along in the permeate flow. One can think that shear induced diffusion, colloidal interaction induced diffusion or lateral migration could lead to distributions in particle velocity in the same way. In the domain of granular flow (as for example in powder flow) where a large number of small particles are arranged in a random way, particle velocity fluctuation was defined by Savage and Jeffrey in 1981 [15] by the term "granular temperature" which quantifies the random motion of particles around the mean velocity. The intensity of distribution used later in this paper could then be linked to the concept of granular temperature and then associated to the dense phase kinetic theory used for the description of the granular flow of particles.

4.1.2. Distribution in permeate velocity

Distributions in solvent velocity can also be responsible for distribution in the radial drag force applied to a particle near the membrane surface. It can be the consequence of heterogeneity of the porous wall. These kinds of heterogeneity have naturally been assumed to be at the origin of a weak form of critical flux [3,7]. As an example, Fig. 8 presents the scanning electron microscope image of a membrane after a latex filtration experiment. Strong changes can be seen in the thickness of the membrane skin (white zone in Fig. 8) which exactly matches a decrease in deposit layer thickness. Areas of membrane surface with high permeability are preferential zones for deposit formation because the local flux is higher: the critical flux may be locally overcome. A porosity heterogeneity inducing important local changes in permeate flux could also lead to the occurrence of the first irreversibility for the same mean permeate flux. In a recent publication, Ognier et al. [16] propose a local change in water flux due to blockage of the first surface pores, which induces an increase in flux through the pores that remain open when operating at constant flux. This kind of phenomenon due to simultaneous mechanisms of pore blocking and cake formation lead to both spatial and temporal dis-

tributions of solvent velocity and then to meet locally the critical conditions for a deposit to form near the membrane surface.

4.1.3. Distribution in critical dispersive velocity (or flux)

Distributions of dispersive critical velocity (or flux) can also occur because of a distribution in surface interaction between the particle and the membrane surface. Local changes in surface charge, in particle size or in roughness can lead to different dispersive forces. As an example, the latex particles used in this work exhibit a size distribution centred on 118 nm with a standard deviation of 20 nm when size analysis (Zetasizer 4, Malvern Inst., UK) is run in monomodally (Gaussian distribution). This dispersion in size can lead to a distribution in drag forces for a given local flux. Critical flux being closely linked to particle stability [2], the particle size distribution can also be responsible for part of the distribution in critical flux observed. The distribution of these properties in a fluid can then lead to a distribution in critical flux.

4.1.4. Summary

As underlined in the previous section, accounting for distribution of critical flux seems to be physically justified. These distributions could be described from different possible physical causes due to multi-body (hydrodynamic or colloidal) interactions and heterogeneous membrane properties. Distributions can act both on the drag force and on the critical dispersive force, which are the two terms of the balance describing critical flux in Eq. (12). However, it seems mathematically equivalent to consider these distributions applied either on the first or on the second member of the force balance for critical flux:

$$F_{\text{drag}} + \langle f'_{\text{drag}} \rangle = F_{\text{disp}} \Leftrightarrow F_{\text{drag}} = F_{\text{disp}} + \langle f'_{\text{disp}} \rangle \qquad (13)$$

i.e. with distributions on the drag force $\langle f'_{\text{drag}} \rangle$ or on the dispersive force $\langle f'_{\text{disp}} \rangle$. The theoretical model previously developed in this paper considers distributions on the dispersive

force, i.e., distribution in critical flux. However, this term of distribution in critical flux accounts more generally for distributions in critical conditions (both fluctuation terms in Eq. (13)) and thus always represents the multiple source of heterogeneity and the complexity of the system. Using a normal (or Gaussian) distribution to represent the distribution of critical flux is justified: this kind of distribution is able to describe diffusive phenomena (based on stochastic process) as well as distribution velocity induced by hydrodynamic interactions [14].

4.2. DCF, critical flux and limiting flux

The results presented in this paper show that distributions in critical flux around a mean critical flux value can explain the occurrence of gradual fouling hence giving an explanation for the weak form of critical flux. *The weak critical flux may then be considered as the consequence of a distribution in strong critical flux*. Furthermore, as presented in Section 3.4, it seems possible to link the experimental critical flux, J_{crit}, to the parameters of the critical flux distribution, $\bar{J}_{crit}$ and σ; where σ is the standard deviation which relates the gap to the strong critical flux concept. If $\sigma = 0$, the strong form of critical flux applies. When σ increases, critical flux becomes less strong and the weak form is a more suitable concept to describe the critical fouling behaviour (as can be seen in Fig. 3). The weak "experimental" critical flux is then preceded by a low fouling zone which is theoretically explained via the DCF model as corresponding to the fouling of areas where the critical flux is much lower than its mean value (existence of zones easier to foul). Furthermore, the weak form of critical flux has been defined [3] as the flux for which a deviation from a linear slope of flux–pressure profile (which can be different from the pure water flux line) occurs. It can be seen that when accounting for the distribution of critical flux around a mean value, one obtains an initial linear variation in "flux versus pressure" differing slightly from that of the water slope. The DCF model then shows its ability to interpret experiments for which the weak form of critical flux was initially developed. Studies using the DCF model to interpret weak-form critical flux data have to be continued before any general conclusions can be drawn as to the impact of critical flux distribution on critical fouling behaviour.

Furthermore, within this model, the limiting flux is defined as the permeate flux for which the probability of having reached critical flux is equal to one: there is no probability to have the membrane working in sub-critical conditions (i.e., without multi-layer deposit). When the initial flux of a run is above the critical flux, the final permeate flux at steady state is assumed to be equal to the critical value. The limiting flux is then linked to an integral of the critical flux distribution giving an expected value of critical flux on the membrane surface. At limiting flux, the overall membrane surface can then be considered as covered by a multi-layer deposit, which increases in thickness as soon as the pressure is increased.

4.3. DFC and phase transition

The critical flux behaviour can be related to a phase transition for the matter accumulated at the membrane surface from a dispersed phase (when mass is accumulated in a concentration polarisation layer) to a condensed (solid or aggregated) phase (when deposit takes place). Critical flux is then defined as process operating conditions leading to the creation on the membrane of an irreversible deposit. From this definition, the term critical finds its physical meaning: i.e., being linked to an irreversible phase transition.

Recent studies in other fields show that phase transitions are not really critical, i.e. with a very sharp change. Spinodal decomposition [17] which leads to an unstable phase is always preceded by a metastable phase (linked to bimodal decomposition). In polymer phase separation, experimental methods provide evidence of microphase separation caused by chemical polydispersity of the copolymers [18]. In crystallisation, results "suggest pre-nucleation density fluctuations, leading to a metastable phase, play an integral role in all three classes of crystallisation" [19]. The use of a distribution in critical flux could be a way to account for the existence of a metastable phase preceding the spinodal decomposition when considering the phase transition leading to the formation of a colloidal deposit on a membrane interface.

4.4. Application of DCF model to the gel theory

Formation of a gel layer could be considered as one of these phase transitions. This analogy has been underlined by a model [13] for the description of gel and deposit formation from the concentration polarisation where critical flux defines both these transitions. The DCF model developed in this paper could then describe the formation of a gel with heterogeneous properties. As a first confirmation of this assumption, the DCF model has been applied to the description of bovine serum albumin (BSA) ultrafiltration [20]. Prior to these ultrafiltration experiments, the membrane was fouled using the BSA solution, in such a way that adsorption during the UF run could be ignored. In the same way as when considering latex filtration, the curve of steady state flux versus TMP can be fully depicted (Fig. 12) by the distribution parameters with, by analogy, a mean critical flux for gel, $\bar{J}_{crit}$, and its standard deviation (Table 3).

Table 3
Value of mean critical flux, $\bar{J}_{crit}$, and its standard deviation, σ, $(\times 10^{-6}\,\mathrm{m\,s^{-1}})$ used to fit BSA filtration experiments with DCF model

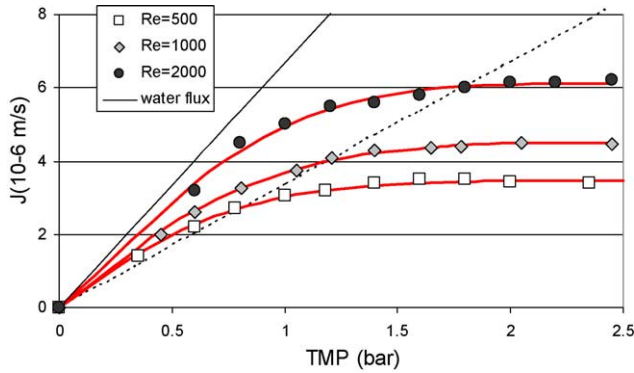|	Critical flux ($\times 10^{-6}\,\mathrm{m\,s^{-1}}$)		
	$Re = 500$	$Re = 1000$	$Re = 2000$
$\bar{J}_{crit}$	2.7	4.0	6.0
σ	4.5	4.8	3.7

Fig. 12. Application of FCFC model to BSA filtration [20]. DCF model (line) allows a very good description of flux–pressure profile (symbols) for various hydrodynamic conditions.

4.5. DCF and fouling complexity

Fouling is a very complex problem. Its complexity is mainly due to the fouling phenomena themselves which deal with high concentration suspensions at a membrane interface which have heterogeneous properties (leading to hydrodynamics, filtration and cross-flow velocity, and transfer, mass accumulation and retention, with a highly non-ideal behaviour). When examining the possible source for critical flux distributions in Section 4.1, it could be wondered if a "direct" model of such complexities is still possible. Using a global distribution covering all sources of complexity could then be a fair and more realistic way to describe fouling. The use of a Gaussian seems well suited to fouling mechanisms where dispersive forces act as diffusion-like motion in this first approach. Furthermore, in this paper we only account for distributions of critical flux and their consequences on steady state filtration. One could think, in a same way, accounting for distributions of critical flux over time to describe transient phenomena in filtration as the permeate flux drift (Pseudo steady state).

5. Conclusions

The consideration of fouling complexity (integrating multiple sources of polydispersity or heterogeneity) allows a very good description of flux-pressure profiles for various colloidal suspensions when fouling is controlled by superficial mechanisms. The permeate flux and its variation with TMP are linked to a distribution function, that can be easily programmed on a spreadsheet. A graphic method is also proposed to determine the function parameters (mean critical flux and standard deviation) from the plot of permeate flux versus trans-membrane pressure.

Considering critical flux distribution allows strong and weak forms of critical flux to be described, then giving a physical interpretation of the often observed weak form, as the consequence on global filtration flux of a distribution in strong form of critical flux. When challenged to experimental

results of cross-flow filtration for latexes or BSA suspensions, the model shows its ability to fully describe experiments with only the two distribution parameters. Furthermore, the experimental critical flux obtained with alternating positive and negative pressure steps seems correlated to the mean critical flux and the standard deviation. Possible explanations for the critical flux distribution in these experiments are supported by a distribution in membrane properties observed on a scanning electron micrograph.

The DCF (distributions of critical flux) model accounting for a distribution in critical flux can be useful to interpret cross-flow filtration experiments, to investigate the effect of suspension properties or membrane materials on fouling and to extrapolate filtration data. The distribution parameters which are the standard deviation and the mean value of critical flux could become a way to depict the effect of critical flux in a "real world" system.

Appendix A. Appendix

Full calculation of the excepted value of critical flux defined by Eq. (5) in the text is based on the following relationship. The integration of the product of the probability density function with the flux can be written in two terms as:

$$\int_0^{j_0} \text{pdf}(j)j\,\mathrm{d}j = \int_0^{j_0} \text{pdf}(j)(j - \bar{j}_{\text{crit}})\mathrm{d}j + \bar{j}_{\text{crit}}(\text{cdf}(j_0) - \text{cdf}(0)) \tag{14}$$

The first term of the preceding equation can be related to the standard deviation as follows:

$$\int_0^{j_0} \text{pdf}(j)(j - \bar{j}_{\text{crit}})\mathrm{d}j = -\sigma^2(\text{pdf}(j_0) - \text{pdf}(0)) \tag{15}$$

Eq. (5) for excepted value can then be rewritten in Eq. (6) by using Eqs. (14) and (15) and the definition of the cumulative distribution function in Eq. (2).

Nomenclature

cdf	cumulative distribution function
D	diffusion coefficient ($m^2\,s$)
E	function for the excepted value ($m\,s^{-1}$)
j	permeate flux (from modelling) ($m\,s^{-1}$)
J	permeate flux (from experiment) ($m\,s^{-1}$)
k	mass transfer coefficient ($m\,s^{-1}$)
L	membrane length (m)
p	probability
pdf	probability density function ($m^{-1}\,s$)
R	hydraulic resistance (m^{-1})
TMP	trans-membrane pressure (Pa)
z	axial length along the membrane (m)

Greek letters

δ	boundary layer thickness (m)
σ	standard deviation ($m\,s^{-1}$)

Subscripts

c	cake
cf	fouling conditions limited by critical flux
crit	critical
lim	limiting
m	membrane
nf	no fouling conditions
ul	unlimited fouling conditions
0	water

References

[1] P. Bacchin, Formation et résistance au transfert d'un dépôt de colloïdes sur une membrane d'ultrafiltration, Ph.D. dissertation, University Paul Sabatier, Toulouse, France, 1994.

[2] P. Bacchin, P. Aimar, V. Sanchez, Model for colloidal fouling of membranes, AIChE J. 41 (1995) 368–376.

[3] R.W. Field, D. Wu, J.A. Howell, B.B. Gupta, Critical flux concept for microfiltration fouling, J. Membr. Sci. 100 (1995) 259–272.

[4] J.A. Howell, Sub-critical flux operation of microfiltration, J. Membr. Sci. 107 (1995) 165–171.

[5] B. Espinasse, P. Bacchin, P. Aimar, On an experimental method to measure critical flux in ultrafiltration, Desalination 146 (2002) 91–96.

[6] D.Y. Kwon, S. Vigneswaran, Influence of particle size and surface charge on critical flux of crossflow microfiltration, Water Sci. Technol. 38 (1998) 481–488.

[7] D.X. Wu, J.A. Howell, R.W. Field, Critical flux measurement for model colloids, J. Membr. Sci. 152 (1999) 89–98.

[8] S-H. Yoon, C-H. Lee, K-J. Kim, A.G. Fane, Three-dimensional simulation of the deposition of multi-dispersed charged particles and prediction of resulting flux during cross-flow microfiltration, J. Membr. Sci. 161 (1999) 7–20.

[9] W.R. Bowen, H.N.S. Yousef, J.I. Calvo, Dynamic cross-flow ultrafiltration of colloids: a deposition probability cake filtration approach, Sep. Purif. Technol. 24 (2001) 297–308.

[10] P. Bacchin, A possible link between critical and limiting flux by consideration of a critical deposit formation along a membrane, J. Membr. Sci. 228 (2) (2004) 237–241.

[11] B. Espinasse, Approche théorique et expérimentale de la filtration tangentielle de colloïdes: flux critique et colmatage, PhD dissertation, University Paul Sabatier, Toulouse, France, 2003 (Available in pdf format by request to authors).

[12] P. Harmant, P. Aimar, Coagulation of colloids retained by porous wall, AIChE J. 42 (12) (1996) 3523–3531.

[13] P. Bacchin, D. Si-Hassen, V. Starov, M.J. Clifton, P. Aimar, A unifying model for concentration polarization, gel-layer formation and particle deposition in cross-flow membrane filtration of colloidal suspensions, Chem. Eng. Sci. 57 (2002) 77–91.

[14] E. Climent, M.R. Maxey, Numerical simulations of random suspensions at finite Reynolds numbers, Int. J. Multiphase Flow 29 (2003) 579–601.

[15] S.B. Savage, D.J. Jeffrey, The stress tensor in a granular flow at high shear rates, J. Fluid Mech. 110 (1981) 255.

[16] S. Ognier, C. Wisniewski, A. Grasmick, Membrane bioreactor fouling in sub-critical filtration conditions: a local critical flux concept, J. Membr. Sci. 229 (1–2) (2004) 171–177.

[17] V.J. Anderson, H.N.W. Lekkerkerker, Insights into phase transition kinetics from colloid science, Nature 416 (2002) 811–815.

[18] C. Konak, R. Bansil, Phase separation in bulk statistical copolymers of styrene and poly(methyl methacrylate), Polymer 39 (24) (1998) 6179–6181.

[19] E.L. Heeley, C.K. Poh, W. Li, Are metastable, precrystallisation, density-fluctuations a universal phenomena? Faraday Discuss. 122 (2003) 343–361.

[20] M. Meireles, Influence de la structure poreuse sur le transfert de solvant et de soluté en ultrafiltration, PhD dissertation, University Paul Sabatier, Toulouse, 1989.